NUCLEAR SCIENCE AND ENGINEERING

DOI: https://doi.org/10.1080/00295639.2020.1819136

Modeling Reactor Noise due to Rod and Thermal Vibrations with Thermal Feedback Using Stochastic Differential Equations

Chen Dubi[a,b]* and Rami Atar[c]

[a]*Nuclear Research Center of the Negev, Physics Department, P.O.B. 9001, Beer Sheva, Israel*
[b]*Ben-Gurion University of the Negev, Department of Mathematics, Beer-Sheva 84105, Israel*
[c]*Technion–Israel Institute of Technology, Viterbi Faculty of Electrical Engineering, Haifa 32000, Israel*

Received February 16, 2020
Accepted for Publication September 1, 2020

Abstract — *Fluctuations associated with power and detector readings in a nuclear reactor, commonly known as reactor noise, are of great importance in nuclear science and engineering. Two different types of noise are described in the literature: internal noise, which is associated with the inherent stochasticity of fission chains, and external noise, which is governed by physical fluctuations of the macroscopic system. The latter may include temperature fluctuations, vibration of regulation rods, fluent turbulence, bubble formation, and more. It is generally true that in power reactors, where high temperatures and strong hydrodynamic flows are characteristic, the external noise is dominant. The goal of this paper is to propose a stochastic differential equation (SDE) that models the effect of two types of external noise terms: the inlet temperature variations, which affect the power through reactivity feedback, and rod vibrations, which affect the reactivity directly. Although these aspects were studied in the past, they were only treated via nonstochastic equations. It is argued that the SDE approach, previously used only for modeling the effect of internal noise on nuclear reactor dynamics, is also highly suitable for modeling external noise. The main advantage of our approach is the ability to arrive at analytic formulas.*

The contributions presented in this paper based on the SDE approach are as follows. Under a linear approximation of thermal feedback, the stabilizing effect of thermal feedback is explained and quantified, and a limiting distribution is analyzed in full. An analysis of the detector response on a finite time interval is carried out, leading to a version of the Feynman variance-to-mean-ratio formula in the presence of external noise. Finally, a calculation of the eigenvalues associated with the linearized system alluded to above is performed, showing that in practical cases the rod vibrations and inlet temperature fluctuations correspond to eigenvalues in distinct timescales. The significance of these finding is discussed.

Keywords — *Reactor noise, stochastic differential equations, rod vibration, inlet temperature fluctuations, thermal feedback.*

Note — *Some figures may be in color only in the electronic version.*

I. INTRODUCTION

Power and detector reading fluctuations in nuclear reactors are commonly known as reactor noise and for decades have been one of the basic topics studied in nuclear science and engineering. Two types of noise are usually considered in the literature. Internal noise is associated with the inherent stochasticity of reactions and fission chains whereas external noise corresponds to physical fluctuations of the macroscopic system.

*E-mail: chendb331@gmail.com

Such fluctuations include temperature fluctuations, vibrations of the regulation rods, fluent turbulence, bubble formation, and more. In general, in power reactors where high temperatures and strong hydrodynamic flows are characteristic, the noise is governed by the external noise while in zero power reactors (ZPRs), the fluctuations are due to internal noises. Therefore, internal noises are sometimes referred to as ZPR noises, and external noises are referred to as power reactor noises.

At present, internal noise measurements are a basic tool in ZPR analysis and are commonly used to determine the kinetic parameters of a subcritical core.[1] External noise measurements, on the other hand, are used for noise diagnostics, aimed to determine the origin of the noise. Because internal and external noises are governed by different physical phenomena, they have traditionally been analyzed by different mathematical tools.[2,3] Under the point model approximation, internal noises are typically analyzed via the probability generating function (PGF) and the so-called master equation.[4] External noises are typically treated in a totally different manner, either by formulating the transfer function and analyzing the effect of a random perturbation in the frequency domain[5] or by the Langevin technique.[3] Some noticeable exceptions are the early work of Harris[6] in 1958, where the PGF approach is adopted; work by Pázsit, where the results are mainly numeric,[2] where a unified model for internal and external noises was proposed (still under the point model approximation) based on the PGF formalism; and work by Pál and Pázsit,[7] where external noises are emulated by assuming a stochastic medium (again, using the PGF formalism).

Under the point model approximation, it is safe to state that internal noises are very well understood. Of course, there is room for improving the existing models to cover spatial effects, dead-time corrections, uncertainty analysis, and many more aspects. However, we have a very clear understanding of the dynamics of internal noises. As for external noises, on the other hand, there are many unresolved issues. An interesting but well-known fact about a critical system (that may be obtained by taking the $k \to 1$ limit of a subcritical system, where k denotes the multiplication factor) is that it might become unstable in the sense that the variance of the steady-state distribution grows linearly with time.[8] Second, we do not have a good understanding of the origin of the noise terms and of their statistical properties. Third, many of the noise terms have spatial dependency, and therefore, it is not clear when the point model is applicable. For these reasons we claim that the precise effect of the different noise sources on the power fluctuations is not yet fully understood under the present state of the art.

In recent years, there has been an effort to model reactor noise as a part of the state equations of the whole dynamical system by appealing to stochastic differential equations (SDEs). We consider the work of Hayes and Allen[9] to be the first to use SDE to model reactor noise (even though the Langevin equation was used in earlier studies on reactor noise; see Ref. 10 and references within). Indeed, Hayes and Allen[9] were the first to analytically derive the intensity of the noise term from first principles and to justify the use of the Brownian motion. Moreover, they were the first to use the tools from Itô calculus to analyze the process. Yet, all the literature so far is dedicated to ZPR noise in a subcritical setting.

The goal of this paper is to propose an SDE-based model that accounts for two types of external noises: the inlet temperature fluctuations, which affect the power through reactivity feedback, and rod vibrations, which affect the reactivity directly. In addition to introducing the model, we analyze its statistical properties and describe possible diagnostic tools.

The paper is organized as follows. In Sec. II we further discuss the difficulties of modeling external noise and describe the contribution of the present study. In Sec. III the SDE model is presented and justified. In Sec. IV some basic statistical properties of the model are studied, and in Sec. VI we discuss through numerical examples the applications of our analysis. Section VII provides concluding remarks.

II. PRELIMINARIES

II.A. Scientific Background I: External Reactor Noises

The topic of power and detection fluctuations due to external noises has long been studied. In 1971, a basic study was presented by Williams[10] in which the external noise was modeled via the Langevin equation in the restricted setting of a subcritical core with a fixed external source and assuming a constant value for the delayed neutron precursors. This approach (which is also studied in Ref. 3) was soon adopted and further developed by many contributors in various directions. In the following decade, the validity of the point model approach was studied by Analytis[11] and Pázsit and Analytis.[12] Saito studied the frequency response to a periodic noise term in the coolant temperature.[13]

One basic challenge in modeling external reactor noise is that the mathematical models lose their stability as the system becomes critical. A critical system differs from a subcritical system in two aspects: the

multiplication factor k becomes unity, and the external source is nullified. As it turns out, if in standard stochastic models we set $k = 1$ and set the external neutron source $S = 0$, the system is stochastically unstable. Moreover, although in a simplified, deterministic mean field model, convergence to a steady-state solution does occur, once the noise term is accounted for, the power variance increases linearly in time, and therefore, it is not possible to consider a steady state. This and related issues to instability were recognized for external noises in Ref. 3 and for internal noises in Ref. 4. Both these standard textbooks mention this phenomenon and consider more or less the same solutions to this issue: The models neglect all power feedback (either physical feedback, such as temperature feedback, or designer feedback, such as the regulation system), which is bound to have a stabilizing effect on the power fluctuations. In a very recent study, it has been shown that in a simplified model, assuming a direct power feedback, any negative feedback will indeed stabilize the system.[14]

Another approach to deal with instability is to add restrictions on the noise term. For example, the system is stabilized if the noise term is filtered through a low-pass filter. Also, filtering the noise term is significant because the sample paths of the solution become smooth, and the equation can be treated as an ordinary differential equation driven by a smooth random noise term, as opposed to an SDE, which may require an Itô correction term (see the treatment in Ref. 10).

In addition to issues of stability, another challenge is that external noises appearing in full-power reactors are much more complicated to model than in ZPRs. In particular, the spatial distribution of the neutrons and the existence of nonlinear feedback are very hard to analyze both in the PGF formalism and via the Langevin technique.

A noticeable effort to model external noises is presented in Ref. 2, where the authors suggest a unified theory for both internal and external noises using the PGF formalism and by assuming a discrete fluctuation on all cross sections in each time interval Δt, which in the limit $\Delta t \to 0$ gives rise to a Wiener process, or white noise term. Their model does not restrict noise frequencies (as in the case of a low-pass filter), but once again, if one assumes a subcritical system (which assures convergence of the steady-state distribution), it will not account for any nonlinear feedback in the system.

In recent years, with growing computation capabilities, we see a growing interest in three-dimensional modeling of external reactor noise using state-of-the-art neutronic and thermodynamic coupled codes.[15–18] These mostly rely on time discretization and do not offer any analytic treatment of the noise propagation or the input/output relation between the noise terms and the state of the system.

The external noises in full-power reactors are governed by macroscopic fluctuations, which eventually change the reactivity of the core, creating power fluctuations. In existing literature, various mechanical processes are studied, including fluctuations in coolant flow, inlet coolant temperature, turbulence and bubble formation in the channels, and control rod vibrations[10] (see also Ref. 19 for a thorough review on the topic). These different types of mechanical processes differ in several aspects. First, each random process may have a different input/output response with the power and is expected to propagate differently. Second, the statistical properties of each process might be different and may affect the core in different amplitudes and frequencies. Third, the appearance of the mechanical vibrations is highly dependent on the type of reactor, and different noise terms may be dominant in different reactor types. It is also important to note that the amplitude of the mechanical vibration might change over time as part of the aging of the reactor. Recent reports indicate power fluctuations of up to 10% in the Kraftwerk Union (KWU)–built pressurized water reactors (PWRs) in Germany.[15]

In the present paper we model two types of external noises: mechanical vibrations of regulation rods and temperature fluctuations of the inlet temperature. The effect of absorber rod vibrations was introduced as early as 1948 (Ref. 20). During the 1970s, the point model was extensively studied, and later, because of the strong spatial dependence of the mechanical vibrations, the problem of identifying the location of the vibrating rod was considered. This involved higher-dimensional analysis (see Ref. 12 and references therein). In recent years, following reports of increasing power vibrations,[15,16] three-dimensional dynamic codes have been used to obtain simulation results for identifying the noise terms. The second type of noise term of interest is the inlet temperature, which is also well studied. Perhaps the most interesting property of temperature oscillations is that the temperature and the power are connected through an inherent feedback loop (see Sec. II.B), and a simple Langevin equation can no longer adequately describe the dynamics of the system. For a linearized system, the transfer function approach is studied in Ref. 13. In a recent publication, the effect of both mechanical rod vibrations and inlet temperature vibrations was analyzed using numeric simulations and compared with experimental results recorded by a KWU-made German reactor.[16,17]

II.B. Scientific Background II: Temperature Feedback

Since the macroscopic cross sections of both the fuel and the moderator depend on temperature and any reactivity change will create a temperature change, the power and the temperature are connected through a feedback loop. The point-kinetics equation with thermal feedback relates the power and delayed neutron precursor concentration, denoted $P(t)$ and $C(t)$, respectively, with fuel temperature $T_f(t)$, channel coolant temperature $T_c(t)$, and inlet temperature $T_i(t)$. The standard relation is give by[21]

$$\begin{cases} \frac{dP}{dt} = \frac{\hat{\rho}-\beta}{\Lambda}P + \lambda C, \\ \frac{dC}{dt} = \frac{\beta}{\Lambda}P - \lambda C, \\ \frac{dT_f}{dt} = \frac{fP}{\mu_f} - \frac{\Omega}{\mu_f}T_f + \frac{\Omega}{\mu_f}T_c, \\ \frac{dT_c}{dt} = \frac{(1-f)P}{\mu_c} + \frac{\Omega}{\mu_c}T_c - \frac{\Omega+2M}{\mu_c}T_c + \frac{M}{\mu_c}T_i, \\ \hat{\rho} = \alpha_f\left(T_{f,0} - T_f\right) + \alpha_c\left(T_{c,0} - T_c\right) + \hat{\rho}_{rod}\ , \end{cases} \tag{1}$$

where the first two equations define the neutron balance and the third and fourth equations define the thermal balance. The last line in Eq. (1) is an equation for $\hat{\rho}$, the deviation from zero reactivity (as a rule, in this paper deviation processes are denoted with a hat, as in $\hat{\rho}$ for reactivity deviations and $\hat{T}$ for temperature deviations; elsewhere in the literature these quantities are often denoted by $\delta\rho$ and δT). The first two terms correspond to reactivity changes due to temperature deviations from the steady state, and the last term, $\hat{\rho}_{rod}$, describes reactivity changes due to the position of the control rods. Often, $\hat{\rho}_{rod}$is the control function and is defined by the control logic.[21] In the present study, this term will be used to describe reactivity perturbations due to vibrations of the control rod.

The system (1) has a steady-state solution defined by three equations. The neutron equilibrium (derived from the first two equations with $\hat{\rho} = 0$) is given by $P_0 = \frac{\Lambda\lambda}{\beta}C_0$, and the thermal equilibrium is defined by a set of equations:

$$\begin{cases} \frac{fP_0}{\mu_f} - \frac{\Omega}{\mu_f}T_{f,0} + \frac{\Omega}{\mu_f}T_{c,0} = 0 \\ \frac{(1-f)P_0}{\mu_c} + \frac{\Omega}{\mu_c}T_{f,0} - \frac{\Omega+2M}{\mu_c}T_{c,0} + \frac{M}{\mu_c}T_{i,0} = 0\ . \end{cases} \tag{2}$$

Equation (2) can be interpreted as a set of equations in four variables: $P_0, T_{f,0}, T_{c,0}$, and $T_{i,0}$, allowing two degrees of freedom. Indeed, the steady state is eventually determined by two operational parameters: the working power and the inlet temperature. Note that the dynamics of inlet temperature is not prescribed in the set of Eq. (1). That is because we assume the second coolant loop, which absorbs heat from the coolant once it exits the channel, is large enough to be considered an infinite sink. In other words, this model assumes that the inlet temperature is fixed (although the fourth equation does assume heat loss from the coolant to the inlet).

II.C. Motivation and Goals

As already stated, the goal of the present study is to construct an SDE model for external noise in power reactors due to rod vibrations and inlet temperature fluctuations. With the very rich literature on the subject, it is important to clarify the contribution and novelty. First, from a modeling point of view, we incorporate both the nonlinear temperature feedback and mechanical rod vibrations in a single framework while giving a physical justification to the use of Brownian motion as the driving term. Second, we show that the use of thermal feedback has a stabilizing effect on the stochastic system: As stated before, in a critical setting the variance of the power grows linearly with time, and a limiting distribution does not exist. Yet, under a linear approximation of thermal feedback, a limiting distribution exists and can be analyzed in full (the stabilization effect of a negative feedback on the mean field deterministic equation is well known and understood). Third, since we analyze our model in the time domain (rather than studying the transfer function), we are able to analyze not only the power in a time epoch but also the detector response on any finite interval. As we will see, this allows us to construct a Feynman variance-to-mean-ratio formula in the context of external noise. Finally, the time domain analysis allows us to compute the eigenvalues of the system of equations, which suggests diagnostic tools for noise analysis. We demonstrate that the rod vibrations and inlet temperature fluctuations correspond to eigenvalues in distinct timescales. The significance of this finding is that the effect of these two causes on the noise can be analyzed by comparing statistical properties of the detection signal in different time regions.

Underlying the approximations offered by the SDE approach is the central limit theorem, according to which only the first and second moments of the primitives are used to form the SDE. In particular, the higher moments

of the primitive processes involved are not reflected in this approximation. Whereas this higher-moment information is lost, it is this simplification that makes the SDE more tractable than exact analysis, allowing for explicit formulas and simplified expressions otherwise. One may think of a hierarchy of tools for analyzing stochastic models in which the SDE approach is located between first-order (or mean field) approximations (using only first-moment information, incorporating no stochasticity, and are thus often considered oversimplified) and exact analysis (often giving rise to problems that are too hard to solve).

III. THE POINT MODEL SDE WITH THERMAL FEEDBACK

The basic model for the point reactor with thermal feedback is given in the set of Eq. (1). For simplicity, it will prove useful to study the relative power and precursor concentration, defined by

$$P_r(t) = \frac{P(t)}{P_0}$$

and

$$C_r(t) = \frac{C(t)}{C_0} \ .$$

In terms of $P_r(t)$ and $C_r(t)$, Eq. (1) can be rewritten as

$$\begin{cases} \frac{dP_r}{dt} = \frac{\hat{\rho}-\beta}{\Lambda} P_r + \frac{\beta}{\Lambda} C_r, \\ \frac{dC_r}{dt} = \lambda P_r - \lambda C_r, \\ \frac{dT_f}{dt} = \frac{fP_0}{\mu_f} P_r - \frac{\Omega}{\mu_f} T_f + \frac{\Omega}{\mu_f} T_c, \\ \frac{dT_c}{dt} = \frac{(1-f)P_0}{\mu_c} P_r + \frac{\Omega}{\mu_c} T_f - \frac{\Omega+2M}{\mu_c} T_c + \frac{M}{\mu_c} T_i, \\ \hat{\rho} = \alpha_f \left(T_{f,0} - T_f\right) + \alpha_c \left(T_{c,0} - T_c\right) + \hat{\rho}_{rod} \ . \end{cases} \tag{3}$$

Recentering gives

$$\begin{cases} \frac{d\hat{P}_r}{dt} = -\frac{\beta}{\Lambda} \hat{P}_r + \frac{\beta}{\Lambda} \hat{C}_r + \frac{\alpha_f \hat{T}_f + \alpha_c \hat{T}_\ell + \hat{\rho}_{rod}}{\Lambda} \left(1 + \hat{P}_r\right), \\ \frac{d\hat{C}_r}{dt} = \lambda \hat{P}_r - \lambda \hat{C}_r, \\ \frac{d\hat{T}_f}{dt} = \frac{fP_0}{\mu_f} \hat{P}_r - \frac{\Omega}{\mu_f} \hat{T}_f + \frac{\Omega}{\mu_f} \hat{T}_c, \\ \frac{d\hat{T}_c}{dt} = \frac{(1-f)P_0}{\mu_c} \hat{P}_r + \frac{\Omega}{\mu_c} \hat{T}_c - \frac{\Omega+2M}{\mu_c} \hat{T}_c + \frac{M}{\mu_c} \hat{T}_i \ , \end{cases} \tag{4}$$

where for each variable Y, $\hat{Y}$ denotes the deviation from the steady-state solution (as described in Sec. II.B).

In standard applications, Eq. (4) is used to model the system response to a reactivity increment $\hat{\rho}$, and the inlet temperature is assumed to be fixed, setting $\Delta\hat{T}_i = 0$. Here, we assume that both $\hat{\rho}_{rod}$ and $\hat{T}_i$ are stochastic processes. An SDE is obtained by further assuming that the set of equations is driven specifically by Brownian motion. Therefore, in what follows we assume both the reactivity variations due to rod vibrations and an inlet temperature having Brownian motion increments. This corresponds to setting (this special indexing is for later use, where it will allow us to simplify notation)

$$\begin{aligned} &\hat{T}_i dt = \sigma_{T_i} dW^{(1)} \\ &\text{and} \\ &\hat{\rho}_{rod} dt = \sigma_{\rho_{rod}} dW^{(4)} \ , \end{aligned} \tag{5}$$

where $W^{(1)}$ and $W^{(4)}$ are two independent Brownian motions.

To justify the use of Brownian motion in our model, recall that the increment of a Brownian motion has a normal distribution and can thus be interpreted as the overall effect of many small independent random variables. For the first equality in Eq. (5), the approximation $\hat{T}_i dt = \sigma_{T_i} dW^{(1)}$ is a commonly used approximation in heat convection (see, for instance, Ref. 22 and references therein). This arises naturally if we consider heat transfer as an average over a large ensemble of minor environmental fluctuations, which are transferred through a spatial diffusion.[22] As for the reactivity term $\frac{\hat{\rho}_{rod}}{\Lambda} dt$, we use an argument similar to that introduced in Refs. 23 and 2. Since the lifetime of a single neutron in the system is an exponential random variable with mean Λ, for an infinitesimal increment of time dt, $\frac{1}{\Lambda} dt$ gives the probability for a neutron to react in the interval $[t, t+dt]$. Since we neglect the internal noises, if we assume $\hat{\rho}_{rod} = 0$, we obtain the deterministic model in which each neutron creates exactly $1-\beta$ neutrons with probability 1. To account for the stochasticity added by the rod vibration, as in Ref. 2, we assume that the deviation in the neutron production (per neutron) $\hat{\rho}_{vib}$ is a discrete random process (the assumption that $\hat{\rho}_{vib}$ is discrete is only for simplification and can easily be dropped) with zero mean and finite variance. We denote $p(\hat{\rho}_{vib} = a) = p_{\hat{\rho}_{vib}}(a)$ and $\sigma^2_{\hat{\rho}_{vib}} = \sum_a p_{\hat{\rho}_{vib}}(a) a^2$ [since it is the deviation from 0, $E(\hat{\rho}_{vib}) = 0$].

In this formulation, the probability for the number of neutrons created by any reacting neutron to deviate from $1-\beta$ by a value of a in the interval $[t, t+dt]$ is given by $p_{\hat{\rho}_{vib}}(a)\frac{1}{\Lambda}dt$. Hence, the deviation from the mean $1-\beta$ is a random variable with 0 mean and variance $\sum_a p_{\hat{\rho}_{vib}}(a)a^2\frac{1}{\Lambda}dt$. As in Ref. 23, we now use a central limit theorem approximation. When considering the huge number of neutrons in the system (which are all independent), the overall deviation from the mean value is a normal random variable with 0 mean and standard deviation $\sqrt{n(t)\sum_a p_{\hat{\rho}_{vib}}(a)a^2\frac{1}{\Lambda}dt}$, where $n(t)$ is the number of neutrons at time t. Finally, if we assume that the power fluctuations are small compared to the working power, then under the square root sign we may take the mean value of the number of neutrons, and we have that for an infinitesimal interval, the random variable $\hat{\rho}_{rod}dt$ has a normal distribution with zero mean and standard deviation $\sqrt{n_0\sigma^2_{\hat{\rho}_{vib}}dt}$.

This formally gives rise to the SDE

$$\begin{cases} d\hat{P}_r = \left(-\frac{\beta}{\Lambda}\hat{P}_r + \frac{\beta}{\Lambda}\hat{C}_r + \frac{\alpha_f\hat{T}_f+\alpha_c\hat{T}_\ell}{\Lambda}\left(1+\hat{P}_r\right)\right)dt \\ \quad +\left(1+\hat{P}_r\right)\frac{\sigma_{\rho_{rod}}}{\Lambda}dW^{(1)}, \\ d\hat{C}_r = \left(\lambda\hat{P}_r - \lambda\hat{C}_r\right)dt, \\ d\hat{T}_f = \left(\frac{fP_0}{\mu_f}\hat{P}_r - \frac{\Omega}{\mu_f}\hat{T}_f + \frac{\Omega}{\mu_f}\hat{T}_c\right), \\ d\hat{T}_c = \left(\frac{(1-f)P_0}{\mu_c}\hat{P}_r + \frac{\Omega}{\mu_c}\hat{T}_c - \frac{\Omega+2M}{\mu_c}\hat{T}_c\right)dt \\ \qquad\qquad + \frac{M\sigma_{T_i}}{\mu_c}dW^{(4)}\ , \end{cases} \tag{6}$$

where $\rho_{rod} = \sqrt{n_0\sigma^2_{\hat{\rho}_{vib}}}$.

Let us emphasize that the use of a Brownian motion increment does not correspond to assumptions made on the statistical properties of rod vibrations or the inlet temperature but is a mere consequence of the fact that both heat convection and fission chains are averaged over a large number of independent identically distributed stochastic increments.

We treat the nonlinear Eq. (6) by linearization. It is achieved by neglecting the second-order terms in $\hat{T}_f\hat{P}_r$ and $\hat{T}_c\hat{P}_r$ [technically, this is achieved by setting $(1+\hat{P}_r)\approx 1$ in the first equation of Eq. (6)]. This is reasonable if we assume that the power fluctuations are much smaller than the working power. Since this study focuses on the steady-state distribution, this assumption is in force (and is considered standard). Thus, we obtain a linear SDE as follows:

$$dX = AXdt + BdW$$

with

$$X = \begin{pmatrix} \hat{P}_r \\ \hat{C}_r \\ \hat{T}_f \\ \hat{T}_c \end{pmatrix};$$

$$A = \begin{pmatrix} -\frac{\beta}{\Lambda} & \frac{\beta}{\Lambda} & \frac{\alpha_f}{\Lambda} & \frac{\alpha_c}{\Lambda} \\ \Lambda & -\Lambda & 0 & 0 \\ \frac{fP_0}{\mu_f} & 0 & \frac{-\Omega}{\mu_f} & \frac{\Omega}{\mu_f} \\ \frac{(1-f)P_0}{\mu_c} & 0 & \frac{f\Omega}{\mu_c} & -\frac{\Omega+2M}{\mu_c} \end{pmatrix};$$

$$B = \begin{pmatrix} \frac{\sigma_{\rho_{vib}}}{\Lambda} & 0 & 0 & 0 \\ 0 & 0 & 0 & 0 \\ 0 & 0 & 0 & 0 \\ 0 & 0 & 0 & \frac{M\sigma_{T_i}}{\mu_c} \end{pmatrix};$$

$$dW_\tau = \begin{pmatrix} dW_\tau^{(1)} \\ dW_\tau^{(2)} \\ dW_\tau^{(3)} \\ dW_\tau^{(4)} \end{pmatrix}, \tag{7}$$

where $dW_\tau^{(i)}, i=1,\ldots,4$ are independent Brownian motion increments. For later use, to allow general formulation, we denote $X=(X_1,X_2,X_3,X_4)^T$ (that is, $\hat{P}_r = X_1, \hat{C}_r = X_2, \hat{T}_f = X_3,$ and $\hat{T}_c = X_4$). Also, we denote the entries of A and B as $(a_{ij})_{i,j=1}^4$ and $(b_{ij})_{i,j=1}^4$, respectively.

IV. STATISTICAL PROPERTIES OF THE REACTOR POWER AND NEUTRON COUNT DISTRIBUTION

IV.A. The Autocorrelation Function

Our first objective is to compute the autocorrelation function of the neutron population process, defined as $\phi_1(s,t) = E[\hat{n}(s)\hat{n}(t)]$. This will allow us to achieve two goals: the computation of the autocorrelation power spectral density and the computation of the first two moments

of the neutron detection count, resulting in the Feynman-Y type of formula.

To this end, for $1 \le j \le 4$, we can write

$$\begin{aligned} X_1(t)X_j(s) &= X_1(t)X_j(t) + X_1(t)X_j(s) \\ &\quad - X_1(t)X_j(t) \\ &= X_1(t)X_j(t) \\ &\quad + X_1(t)\big(X_j(s) - X_j(t)\big) \\ &= X_1(t)X_j(t) \\ &\quad + X_1(t)\int_t^s dX_j(\tau) \\ &= X_1(t)X_j(t) \\ &\quad + X_1(t)\int_t^s \sum_{i=1}^4 a_{i,j}X_j(\tau)d\tau \\ &\quad + X_1(t)\int_t^s \sum_{i=1}^4 b_{i,j}(\tau)dW_\tau^{(i)} \, . \end{aligned} \tag{8}$$

Denote $\phi_i(s,t) = E[X_i(s)X_1(t)]$. Taking expectation,

$$\begin{aligned} \phi_i(s,t) &= \phi_i(t,t) + \int_t^s \sum_{j=1}^4 a_{i,j}\phi_j(\tau,t)d\tau \\ &\quad + E\left[X_1(t)\int_t^s \sum_{i=1}^4 b_{i,j}(\tau)dW_\tau^{(i)}\right] \, . \end{aligned}$$

Since for $\tau \ge t$ and $u \ge 0$, $X_1(t)$ and $W_{\tau+u}^{(i)} - W_\tau^{(i)}$ are independent and $E[W_{\tau+u}^{(i)} - W_\tau^{(i)}] = 0$, the last term vanishes, and thus for $s > t$, $\phi_i$satisfies the equation

$$\frac{d\phi_i(s,t)}{ds} = \sum_{j=1}^4 a_{i,j}\phi_j(s,t) \, ,$$

with the initial condition

$$\phi_j(t,t) = E\big[X_1(t)X_j(t)\big] \, .$$

The autocorrelation vector $\Phi(s,t) = [\phi_1(s,t), \phi_2(s,t), \phi_2(s,t), \phi_4(s,t)]^T$ then satisfies the linear equation

$$\frac{d\Phi(s,t)}{ds} = A\Phi(s,t) \, ,$$

where A is exactly the same state matrix as in Eq. (7) and the initial condition is given at $s = t$ by

$$\Phi(t,t) = \begin{pmatrix} E[X_1(t)X_1(t)] \\ E[X_1(t)X_2(t)] \\ E[X_1(t)X_3(t)] \\ E[X_1(t)X_4(t)] \end{pmatrix} \, .$$

The solution, for $s \ge t$, is given by

$$\Phi(s,t) = e^{(s-t)A}\Phi(t,t) \, . \tag{9}$$

To obtain an explicit solution, our next order of business is to compute $\Phi(t,t)$. Since we are interested in the steady-state distribution, we compute in Sec. IV.B the limit $\Phi_\infty = \lim_{t\to\infty}\Phi(t,t)$.

IV.B. The Covariance Matrix of *X*

The covariance matrix of X is defined by $S = E[XX^T]$. Under the assumption that $W^{(1)}$ and $W^{(4)}$ are independent, $S(t)$satisfies the Lyapunov equation[24]

$$\frac{dS}{dt} = SA^TA + A^TAS + B^TB \, . \tag{10}$$

If the matrix A is stable (which is always the case if the thermal feedback is negative), then S converges to a steady-state solution S_∞, satisfying the algebraic Lyapunov equation

$$S_\infty A^TA + A^TAS_\infty + B^TB = 0 \, . \tag{11}$$

For Eq. (11), it is well known that under the assumption that A is stable, it has a unique solution given by[24]

$$S_\infty = \int_0^\infty e^{A^TAt}B^TBe^{A^TAt}dt \, . \tag{12}$$

Equation (12) is considered a classical explicit solution, but in practice, numeric solutions are often more efficient.

Note that the first column of S_∞ is exact when defining $\lim_{t\to\infty}\Phi(t,t) = \Phi_\infty$. Since the stability of A is a necessary condition for the existence of a limiting solution to Eq. (10), Eq. (12) is a full description of the initial condition to the correlation

function, as defined in Eq. (9). If we denote the first column of the matrix with S^1_∞ (9), then for $s \geq t$, the autocorrelation function is given by

$$\Phi(s,t) = e^{(s-t)A} S^1_\infty \ .$$

Focusing only on $\phi_1(s,t)$, we may write in a more explicit form

$$\phi_1(s,t) = \sum_{j=1}^{4} c_j e^{\mu_j (s-t)} \ , \tag{13}$$

where $\{\mu_j\}_{j=1}^4$ is the eigenvalue of A and $\{c_j\}$ is constant. We shall neglect the possibility that A has an eigenvalue with multiplicity higher than 1. This is justified by the fact that the condition for an eigenvalue with multiplicity higher than 1 is nonstable and is lost under small perturbations in the numeric parameters.

V. INTEGRAL REPRESENTATION OF THE NEUTRON COUNT

In Sec. IV we have computed the correlation function of the power (or, equivalently, the neutron population size), which is the basic physical property we are studying. While this function is an often used tool, it has two shortcomings. First, it is often statistically very hard to sample, and the sampling is done through the Fourier transform of the signal, which leads to additional uncertainties.[25] Second, in practice, the power is not truly measurable. Instead, to directly estimate the power (not through the temperature of the outlet coolant), we measure neutron detections that are never defined in a time epoch but always over finite intervals. Therefore, our next objective is to analyze the count distribution in a time interval of duration T. We assume that the system is in a steady state; hence, the count distribution is only a function of T and not the actual start/end point detection interval.

In deterministic models, it is usually assumed that the number of detections is a linear function of the population size. In stochastic modeling the relation between the two is more delicate. The power stochastic process, and in addition the detection process, is related to the power via further stochasticity. Assuming a point model, the probability for detection of each neutron is fixed, and we denote the detection probability (per time unit per power unit) by λ_d. When modeling internal noises, the detection process affects the population size since a detected neutron is absorbed. For external noise, since the system is not at zero power, the detector is more likely to be out of the core (otherwise, it will be saturated), and the detected neutrons are already on the peripheral regions. As a result, absorption of the neutron has a very small, if any, influence on the dynamics of the core (see remarks below for further details).

The goal of this section is to obtain formulas for the first two moments of the count distribution in an interval of duration T, in terms of the autocorrelation function $\Phi(s,t)$, assuming steady state. The detection interval is $[0,T]$. Denote by $D(T)$ the number of detections in $[0,T]$.

Our approximation is based on considering infinitesimal values of dt and assuming that conditioned on $P(t)$, the number of detections in the interval $[t, t+dt]$, denoted $D_{[t,t+dt]}$, is a Bernoulli random variable with parameter $P(t)\lambda_d dt$ [notice that $P(t)$ is a random variable]. As a result we may write $E\left[D_{[t,t+dt]}|P(t)\right] = P(t) \quad \lambda_d dt + O(dt^2)$and $\mathrm{Var}\left[D_{[t,t+dt]}|P(t)\right] = P(t)\lambda_d dt(1-\lambda_d dt) + O(dt^2) = P(t)\lambda_d dt + O(dt^2)$..

Now, we partition the interval $[0,T]$ into N consecutive intervals of duration dt, with $N = \frac{T}{dt}$; set $t_n = n\,dt$ for $n = 0, ..., N$; and let D_n denote the number of detections in the interval $[t_{n-1}, t_n]$ (hence, $D_n = D_{[t_n, t_n+dt]}$). Clearly, we may write$D(T) = \sum_{n=1}^{N} D_n$.

For the first moment we have

$$\begin{aligned} E[D(T)] &= E\left[\sum_{n=1}^{N} D_n\right] \\ &= \sum_{n=1}^{N} E[E[D_n|P(t_n)]] \\ &= \sum_{n=1}^{N} P_0 \lambda_d dt + O(dt^2) \ , \end{aligned} \tag{14}$$

and as $N \to \infty$, we have

$$E[D(T)] = \int_0^T \lambda_d P_0 dt = \lambda_d P_0 T \ . \tag{15}$$

For the second moment, using the complete variance formula, we have

$$\begin{aligned}\mathrm{Var}[D(T)] &= \mathrm{Var}\left[\sum_{n=1}^{N} D_n\right] \\ &= E\left[\mathrm{Var}\left[\sum_{n=1}^{N} D_n|P(t_n)\right]\right] \\ &\quad + \mathrm{Var}\left[E\left[\sum_{n=1}^{N} D_n|P(t_n)\right]\right] .\end{aligned}$$

For the second term above, using the same argument used for the mean, as $N \to \infty$, we have

$$\begin{aligned}&\lim_{N\to\infty} \mathrm{Var}\left[E\left[\sum_{n=1}^{N} D_n|P(t_n)\right]\right] \\ &= \lambda_d^2 \mathrm{Var}\left[\int_0^T \hat{P}(t)dt\right].\end{aligned}$$

For the first term, since for fixed values of $P(t_n)$ and $P(t_m)$, D_n and D_m are independent ($n \neq m$), we have that $\mathrm{Var}\left[\sum_{n=1}^{N} D_n|P(t_n)\right] = \sum_{n=1}^{N} \mathrm{Var}[D_n|P(t_n)] = \sum_{n=1}^{N} P(t_n)\lambda_d dt + O(dt^2)$; hence,

$$\begin{aligned}&\lim_{N\to\infty} E\left[\mathrm{Var}\left[\sum_{n=1}^{N} D_n|P(t_n)\right]\right] = \int_0^T \lambda_d P_0 dt \\ &= \lambda_d P_0 T\end{aligned}$$

and

$$\begin{aligned}\mathrm{Var}[D(T)] &= \lambda_d^2 \mathrm{Var}\left[\int_0^T \hat{P}(t)dt\right] \\ &\quad + \lambda_d P_0 T \ . \end{aligned} \tag{16}$$

To analyze the first term above,

$$\begin{aligned}\mathrm{Var}\left[\int_0^T \hat{P}(t)dt\right] &= E\left[\left(\int_0^T \hat{P}(t)dt\right)^2\right] \\ &= P_0^2 E\left[\left(\int_0^T \hat{P}_r(t)dt\right)^2\right].\end{aligned}$$

Next,

$$\begin{aligned}&E\left[\left(\int_0^T \hat{P}_r(t)dt\right)^2\right] \\ &= E\left[\left(\int_0^T \hat{P}_r(t)dt\right)\left(\int_0^T \hat{P}_r(s)ds\right)\right] \\ &= E\left[\int_0^T\int_0^T \hat{P}_r(t)\hat{P}_r(s)dtds\right] \\ &= \int_0^T\int_0^T E\left[\hat{P}_r(t)\hat{P}_r(s)\right]dtds \\ &= \int_0^T\int_0^T \phi_1(s,t)dtds \\ &= 2\int_0^T\int_s^T \phi_1(s,t)dtds \ . \end{aligned} \tag{17}$$

Substituting the expression for the autocorrelation from Eq. (13) in Eq. (17), Eq. (16) reads

$$\begin{aligned}\mathrm{Var}[D(T)] &= P_0^2\lambda_d^2 2\sum_{j=1}^{4} c_j \int_0^T\int_s^T e^{\mu_j(t-s)}dtds \\ &\quad + \lambda_d P_0 T \\ &= P_0^2\lambda_d^2 2\sum_{j=1}^{4} c_j \int_0^T e^{-\mu_j s}\int_s^T e^{\mu_j t}dtds + \lambda_d P_0 T \\ &= P_0^2\lambda_d^2 2\sum_{j=1}^{4} \frac{c_j}{\mu_j}\int_0^T \left[e^{\mu_j(T-s)} - 1\right]ds + \lambda_d P_0 T \\ &= P_0^2\lambda_d^2 2\sum_{j=1}^{4} \frac{c_j T}{-\mu_j}\left(1 - \frac{1-e^{\mu_j T}}{-\mu_j T}\right) \\ &\quad + \lambda_d P_0 T \ , \end{aligned} \tag{18}$$

which is the main result of this section.

We can further compute the variance-to-mean ratio (or the Feynman-Y function), defined by

$$Y(T) = \frac{\mathrm{Var}[D(T)]}{E[D(T)]} - 1 \ .$$

The expression obtained is as follows:

$$Y(T) = 2P_0\lambda_d \sum_{j=1}^{4} \frac{c_j}{-\mu_j}\left(1 - \frac{1-e^{\mu_j T}}{-\mu_j T}\right) \ . \tag{19}$$

It is interesting to note that this expression is very similar to the classical Feynman-Y formula in a subcritical setting (with a single delayed neutron group) but with two more modes, associated with the system feedback. From a theoretical viewpoint, Eq. (19) sets the ground for noise experiments in a critical setting, as described in Sec. VI.

VI. EXAMPLES AND APPLICATIONS

The above development focuses on theoretical aspects of the problem, from modeling to analytic expressions. In what follows we consider the practical aspects of the model introduced, addressing the question of what one learns about the system by sampling the first two moments of the count distribution. We will suggest an analogy to the classic Feynman-α experiment, with two goals: measuring the delayed neutron fraction, and noise diagnostics.

VI.A. Some Practical Considerations

A very interesting feature of Eqs. (18) and (19) is the fact that the exponential modes do not depend on the noise amplitude. The exponential modes are simply the eigenvalues of A, which is independent of σ_T and σ_{vib}. Of course, this is not to say that the variance does not depend on the noise amplitude: The coefficients have a strong dependence on both σ_T and σ_{vib}. We study the matrix A carefully, assuming that the feedback term is sufficiently small (with respect to β) to be considered as a perturbation. In this case the unperturbed system is extremely simple: It has exactly two eigenvalues: $-\left(\frac{\beta}{\Lambda}+\lambda\right)$ is an eigenvalue of multiplicity 1, and 0 is an eigenvalue of multiplicity 3. As a result, we expect that out of the four eigenvalues $\{\mu_i\}_{i=1}^4$, one (which we may assume is μ_1) would be a perturbation of $-\left(\frac{\beta}{\Lambda}+\lambda\right)$, and the other three would be perturbations of 0 (and since the feedback is negative, all eigenvalues would have a negative real part). If $-\left(\frac{\beta}{\Lambda}+\lambda\right)$ is sufficiently larger than 0, this means that both the autocorrelation function and the Feynman-Y function have a distinctive behavior in different timescales. That is, if $0 < t < 1/\mu_1$, then we may assume that $e^{\mu_k t}, k = 2,3,4$ are constants, and we have a single exponential mode (with a possible direct-current offset), and if $1/\mu_1 \ll t < \min(1/\mu_k, k = 2,3, \quad 4) \rightarrow$, the first exponent will vanish. Moreover, since the first eigenvalue μ_1 is not associated with the thermal feedback, we expect that the coefficient c_1 will be more dominant as σ_{vib} is dominant while $c_2, c_3,$ and c_4 will have a stronger effect as σ_T grows.

As for the Feynman-Y function, we may write

$$Y(T) = \sum_{j=1}^{4} Y_{\infty,j}\left(1 - \frac{1-e^{\mu_j T}}{-\mu_j T}\right) \ ,$$

where the first mode $Y_{\infty,1}\left(1 - \frac{1-e^{\mu_1 T}}{-\mu_1 T}\right)$ is associated with the rod vibration and corresponds to timescales of $1/\mu_1$ and the last three modes $\sum_{j=2}^{4} Y_{\infty,j}\left(1 - \frac{1-e^{\mu_j T}}{-\mu_j T}\right)$ are associated with the temperature vibrations and correspond to timescales of $1/\mu_k, k = 2,3,4$.

VI.B. Numerical Results

VI.B.1. Simulation Parameters

To validate our results and understand the possible diagnostic tools at hand, two numerical simulations were conducted differing in σ_T and σ_{vib}. Both simulations used kinetic parameters typical for a Three Mile Island (TMI)–type PWR power reactor, taken from Ref. 21. These parameters are typical for the middle of the burnout cycle. The complete numerical parameters are given in Table I.

For the first simulation, we have taken $\sigma_{vib} = 2$ (pcm) and $\sigma_T = 0.5$ (°C), and for the second simulation, we have taken $\sigma_{vib} = 0.5$ (pcm) and $\sigma_T = 4$ (°C). The working power was set at 2500 MW, and the mean inlet temperature was set at 150°C.

The numerical simulation was done using the Euler-Maruyama method,[26] but since the power and temperature gradient have very different timescales, the equation is stiff, and the drift was estimated using a fourth-order

TABLE I

Kinetic Parameters for Simulation

β 0.006019	Λ 0.00002 (s)	α_f -0.0000324 $(\frac{\hat{\rho}}{^\circ C})$	μ_f 26.3 (MW/°C)	Ω 6:6 (MW)
λ 0.15(L/s)	α_c -0.000213 $(\frac{\hat{\rho}}{^\circ C})$	μ_c 71.8 (MWs°C)	M 102 (MW/°C)	f 0.92

Runge-Kutta approximation. The time increment used in the simulation was taken to be equal to the generation time, $\Delta t = 2 \times 10^{-5}$(s). A total of 10^7 steps was considered, simulating a 200-s measurement.

The power simulation series resulted in $\{P(t_i)\}_{i=1}^{10^7}$, indicating the power at time t_i (with resolution of 2×10^{-5} s). To simulate the detector response, one must also sample in each step the number of detections. Let us assume that the value of λ_d is $40[1/(\text{sMW})]$, which is equivalent to 10^4 counts/s. Ideally, the number of detections in each interval $[t_i, t_{i+1}]$ would be sampled by using a binomial distribution with parameters $P(t_i)$ and $\lambda_d dt$. However, this is not practical from a computational point of view. With such a large value of $P(t_i)$ (on the order of 2500), a normal approximation for the binomial is accurate. Therefore, in each interval, the number of detections was sampled using a normal distribution with an average value $P(t_i)\lambda dt$, and standard deviation $\sqrt{P(t_i)(1 - P(t_i)\lambda_d dt)\lambda_d dt}$. The detector response simulation resulted with a series $\{D(t_i)\}_{i=1}^{10^7}$, indicating the number of detections in the interval $[t_i, t_{i+1}]$.

VI.B.2. Simulation Results

The simulation results, in terms of $\hat{P}_r$, are shown in Figs. 1 and 2. The standard deviation of the simulated values is given in Table II.

In Table II we see that the standard deviation of the power is very close in both simulations. However, in Figs. 1 and 2, a very different behavior can be seen: In the first simulation,

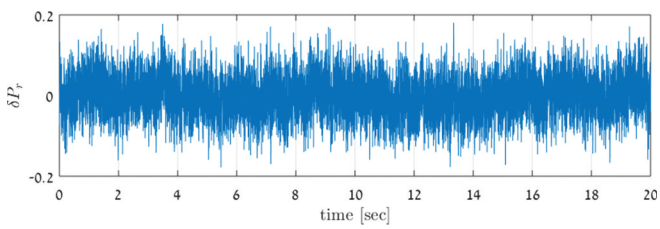

Fig. 1. Simulation 1: Relative power fluctuations δP_r (as a function of time) induced by rod vibration $\sigma_{vib} = 2$ (pcm) equivalence and $\sigma_T = 0.5$ (°C).

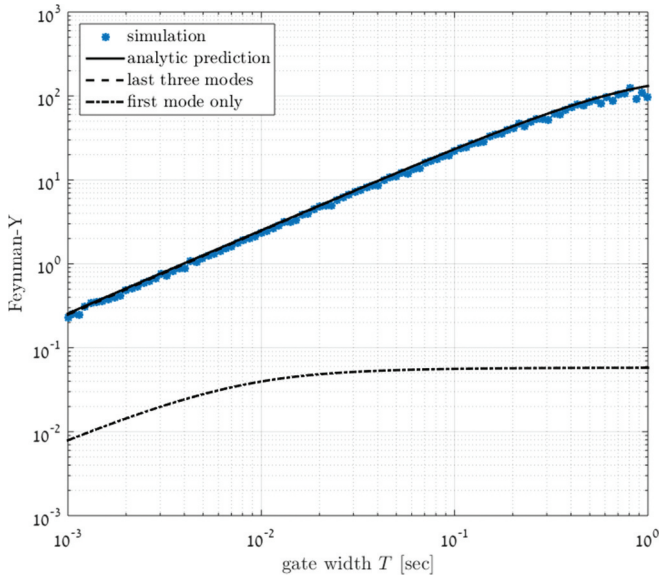

Fig. 2. Simulation 2: Relative power fluctuations δP_r (as a function of time) induced by rod vibration $\sigma_{vib} = 0.5$ (pcm) equivalence and $\sigma_T = 4$ (°C).

where the rod vibrations are more significant, we observe very fast fluctuations, while in the second simulation, where the temperature has a more significant effect, we see a second timescale in the vibration, which is much slower. In terms of the autocorrelation function, this means that the last three eigenvalues are much more dominant in the second simulation.

The eigenvalues of the matrix A are given by

$$\mu_1 = -300.53,$$
$$\mu_2 = -1.2794,$$
$$\mu_3 = -0.9235,$$

and

$$\mu_4 = -0.1303.$$

TABLE II

Simulated Standard Deviations

	$\sigma_{\hat{P}_r}$ (%)	$\sigma_{\hat{C}_r}$ (%)	$\sigma_{\hat{T}_l}$ (°C)	$\sigma_{\hat{T}_f}$ (°C)
Simulation 1 [$\sigma_{vib} = 2$(pcm); $\sigma_T = 0.5$(°C)]	4.36	0.14	0.75	0.39
Simulation 2 [$\sigma_{vib} = 0.5$(pcm); $\sigma_T = 4$(°C)]	4.9	0.67	3.19	1.4

TABLE III

Coefficient of the Autocorrelation Function

	c_1	c_2	c_3	c_4
Simulation 1 [$\sigma_{vib} = 2$(pcm); $\sigma_T = 0.5$(°C)]	16×10^{-4}	4.9×10^{-4}	3.9×10^{-4}	6.7×10^{-7}
Simulation 2 [$\sigma_{vib} = 0.5$(pcm); $\sigma_T = 4$(°C)]	8×10^{-5}	7.8×10^{-3}	5.3×10^{-3}	1×10^{-5}

As expected, it is seen that the first eigenvalue is a small perturbation of $-\left(\frac{\beta}{\Lambda}+\lambda\right) = -301.1$ and that the last three eigenvalues are two and three orders of magnitude smaller than the first. Tables III and IV give the coefficients of the calculated autocorrelation and Feynman-Y function.

Figures 3 and 4 show the Feynman-Y curves, both simulation and analytic estimations, for the two experiments.

The simulated Feynman-Y curve was obtained in a straightforward manner. A total of 100 values of T were taken in a logarithmic scale in the interval $10^{-3} \leq T \leq 1$.

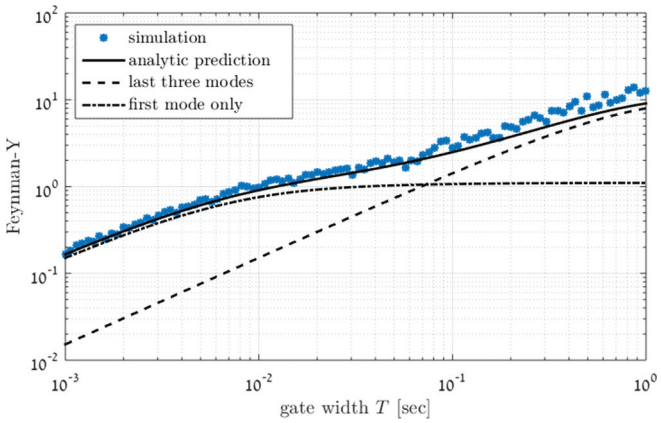

Fig. 3. Feynman-Y plot (simulation and analytic prediction) for simulation 1. For relative short gates ($T < 10^{-2}$), the functional behavior is dominated by the first exponential mode, associated with the rod vibration, and in relative long gates ($T > 10^{-1}$), the functional behavior is dominated by the last three exponential modes, associated with the temperature vibration.

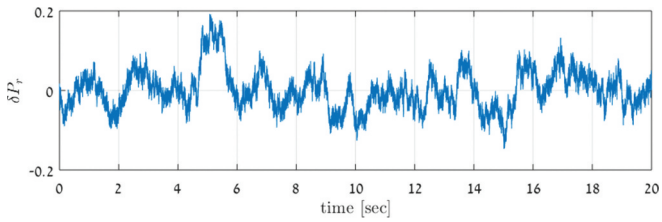

Fig. 4. Feynman-Y plot (simulation and analytic prediction) for simulation 2. The functional behavior is dominated by the last three exponential modes, associated with the temperature vibration.

For each gate width T, the detection signal was divided into N_T consecutive gates, starting at $\{t_j\}_{j=1}^{N_T}\}$, and the number of detections in the interval $[t_j, t_j + T]$ is given by $\sum_{\ell=0}^{k-1} D(t_{j+\ell})$, where $\{D(t_i)\}_{1=1}^{10^7}$ is the detector response simulation and $k = T/dt$. From here, the mean and the variance were estimated in a standard manner. The analytic prediction for $F(Y)$ is exactly as described in Eqs. (13) and (19). The eigenvalues $\{\mu_i\}_{i=1}^{4}$ of A were calculated numerically. To compute the coefficients $\{c_i\}_{i=1}^{4}$, we make use of the fact that if $\{\mu_i\}_{i=1}^{4}$ are the eigenvalues of A, and D is the matrix whose columns are the corresponding eigenvectors, then

$$e^{At} = D \begin{pmatrix} e^{\mu_1 t} & 0 & 0 & 0 \\ 0 & e^{\mu_2 t} & 0 & 0 \\ 0 & 0 & e^{\mu_3 t} & 0 \\ 0 & 0 & 0 & e^{\mu_3 t} \end{pmatrix} D^{-1}.$$

The coefficients $\{c_i\}_{i=1}^{4}$ were computed after the solution to the Lyapunov Eq. (11), and the eigenvector matrix D and its inverse were computed numerically.

We emphasize that the numerical simulations did not assume any linear approximation. Figures 3 and 4 also show the first mode of the calculated Feynman-Y function, and the last three modes (together) as well.

The most important result is that there is very good agreement between the analytic prediction and the simulation results. Another point to notice is that there is a very distinctive qualitative difference between the two simulations. In the second experiment, the Feynman-Y curve is completely dominated by the last three modes (this is also noticeable in Table IV). In the first experiment, there is a small range near the origin (roughly $10^{-3} \leq T \leq 10^{-2}$, where the Feynman-$Y$ curve is dominated by the first mode alone. Then, as the gate width T increases, the influence of the last three modes grows.

These results agree with intuition. Indeed, mechanical vibrations of a control rod have an immediate effect on the power, which translates into very high-frequency noises on the power. However, temperature vibrations of the second circle take time to propagate to the core, where the timescales are now dictated by the heat transfer rate between the fuel and the coolant and the flow rate of the coolant, a process that takes much longer than the generation time.

Most importantly, our results indicate that when external noise is dominant, sampling the noise-to-source ratio in a full-power reactor can serve as a diagnostic tool toward identifying the origin of the noise term. The fact that the two types of external noises examined propagate in very different timescales and that this difference can be quantified through the stochastic point-kinetics equation suggests an approach to noise diagnostics in critical cores via techniques similar to those used in ZPRs. Potentially, it may even lead to quantification of the delayed neutron fraction and the feedback coefficients.

VII. CONCLUDING REMARKS

The goal of this study was to suggest a new model based on SDE to address external noise in full-power reactors. The use of SDE driven by Brownian motion was justified by the diffusive nature of both heat transfer and neutron transport. The model assumes point reactor kinetics and considers two types of noises: temperature fluctuations on the inlet temperature and mechanical vibrations of the control rods. One of the contributions that to the best of our knowledge was never addressed earlier in the context of stochastic transport is the incorporation of the thermal feedback into the dynamics. As we showed, adding the thermal feedback had two benefits: The model is closer to the actual physical phenomenon, and this feedback serves to stabilize the state, resulting in finite variance for the power fluctuations.

The results indicate that the autocorrelation function, as well as the variance-to-mean ratio, is governed by four experiential modes: the first mode, which is associated with the rod vibration, is characterized by very short timescales, and the other three modes, associated with the temperature fluctuations, are characterized by long timescales. The analytic results were compared with numerical simulations, using kinetic parameters of a TMI-type reactor, showing high correspondence. Moreover, the results indicate that the different timescales in the model, which were fully quantified by the analytic predictions, may serve to discriminate between contributions of rod vibrations to the noise and contributions of temperature fluctuations.

The use of noise experiments in power reactors, aimed at noise diagnostics and experimental measurements of kinetic parameters, is an appealing idea. However, before the theory introduced in this work can be implemented, there are crucial questions that must be addressed, such as the following:

1. *Limitations of the point model*: In measuring internal noises, it is well established that the point model gives a good description of the detector response. In external noises, since the noises are often local, the point model must be further validated. Future works should include spatial generalization, or coupling of the proposed equation with a steady-state Boltzmann equation, to compensate for spatial effects.

TABLE IV

Coefficients of the Feynman-Y Function

	$Y_{\infty,1}$	$Y_{\infty,2}$	$Y_{\infty,3}$	$Y_{\infty,4}$
Simulation 1 [$\sigma_{vib} = 2$(pcm); $\sigma_T = 0.5$(°C)]	1.1	77.3	− 74.3	1.03
Simulation 2 [$\sigma_{vib} = 0.5$(pcm); $\sigma_T = 4$(°C)]	0.057	1.22×10^3	-1.15×10^3	16.2

2. *Control rod motion*: One element that we did not cover in our model and is always a part of the reactor is the regulation system. The regulation system is designed to compensate any power drift and operates on very different—in fact much longer—timescales than stochastic rod vibrations.

The above issues need further planning in the future.

NOMENCLATURE

α_c = coolant temperature reactivity coefficient $(\frac{\Delta k/k}{^\circ C})$

β = delayed neutron fraction

α_f = fuel temperature reactivity coefficient $(\frac{\Delta k/k}{^\circ C})$

f = fraction of reactor power deposited in the fuel

Ω = fuel-to-coolant heat transfer coefficient (MW/°C)

μ_f = heat capacity of the fuel $(\frac{MWs}{^\circ C})$

μ_c = heat capacity of the coolant $(\frac{MWs}{^\circ C})$

M = mass flow rate times heat capacity of the coolant (MW/°C)

λ = neutron generation time (s)

P_0 = reactor power (MW)

References

1. R. E. UHRIG, *Random Noise Techniques in Nuclear Reactor Systems*, Ronald Press (1970).
2. I. PÁZSIT, Z. F. KUANG, and A. PRINJA, "A Unified Theory of Zero Power and Power Reactor Noise via Backward Master Equations," *Ann. Nucl. Energy*, **29**, *2*, 169 (2002); https://doi.org/10.1016/S0306-4549(01)00029-9.
3. M. M. R. WILLIAMS, *Random Processes in Nuclear Reactors*, Pergamon Press (1974).
4. I. PÁZSIT and L. PÁL, *Neutron Fluctuations: A Treatise on the Physics of Branching Process*, Elsevier Print (2008).
5. T. YAMAMOTO, "Implementation of a Frequency-Domain Neutron Noise Analysis Method in a Production Level Continuous Monte Carlo Code: Verification and Applications in a BWR," *Ann. Nucl. Energy*, **115**, 494 (2018); https://doi.org/10.1016/j.anucene.2018.02.008.
6. D. R. HARRIS, "Stochastic Fluctuations is a Power Reactror," WAPD-TM-290, U.S. Atomic Energy Commission (1958).
7. L. PÁL and I. PÁZSIT, "Theory of Neutron Noise in a Temporally Fluctuating Multiplying Medium," *Nucl. Sci. Eng.*, **155**, *3*, 425 (2007); https://doi.org/10.13182/NSE07-A2674.
8. M. A. RODRIGUEZ and L. PESQUERA, "Stability Analysis of Linear Reactor Systems with Reactivity Fluctuations," *J. Nucl. Sci. Technol.*, **21**, *10*, 797 (1984); https://doi.org/10.1080/18811248.1984.9731115.
9. J. HAYES and E. ALLEN, "Stochastic Point-Kinetic Equations in Nuclear Reactor Dynamics," *Ann. Nucl. Energy*, **32**, 572 (2005); https://doi.org/10.1016/j.anucene.2004.11.009.
10. M. M. R. WILLIAMS, "The Kinetic Behaviour of Simple Neutronic Systems with Randomly Fluctuating Parameters," *J. Nucl. Eng.*, **25**, 563 (1971); https://doi.org/10.1016/0022-3107(71)90051-7.
11. G. TH. ANALYTIS, "Investigation of the Space-Dependent Global Component of the Neutron-to-Inlet Coolant Temperature Fluctuations Transfer Function," *Ann. Nucl. Energy*, **5**, 597 (1978).
12. I. PÁZSIT and G. TH. ANALYTIS, "Theoretical Investigation of the Neutron Noise Diagnostics of the Two-Dimensional Control Rod Vibrations in PWR," *Ann. Nucl. Energy*, **7**, *3*, 171 (1980); https://doi.org/10.1016/0306-4549(80)90082-1.
13. K. SAITO, "Analytical Study of Operating Reactor Noise on a Single Channel and Single Phase Flow Model," *J. Nucl. Sci. Technol.*, **10**, *5* (1973).
14. G. STEIN and C. DUBI, "Stabilization of the Stochastic Point Reactor Kinetics Equation Through Power Feedback," *Eur. Phys. J. Plus*, **135** (2020); https://doi.org/10.1140/epjp/s13360-020-00215-z.
15. U. ROHDE et al., "Neutron Noise Observation in German KWU Built PWRs and Analyses with the Reactor Dynamics Code DYN3D," *Ann. Nucl. Energy*, **112**, 715 (2018); https://doi.org/10.1016/j.anucene.2017.10.033.
16. D. CHIONIS et al., "PWR Neutron Noise Phenomenology: Part I—Simulation of Stochastic Phenomena with SIMULATE-3K," *Proc. PHYSOR 2018*, Cancun, Mexico, April 22–26, 2018.
17. D. CHIONIS et al., "PWR Neutron Noise Phenomenology: Part II—Qualitative Comparison Against Plant Data," *Proc. PHYSOR 2018*, Cancun, Mexico, April 22–26, 2018.
18. H. MALMIR and N. VOSOUGHI, "Neutron Noise Induced by Fluctuations of the Boric Acid Content in Pressurized Water Reactors," *Proc. PHYSOR 2014*, Kyoto, Japan, September 28–October 3, 2014.
19. K. SAITO, "Source Papers in Reactor Noise," *Prog. Nucl. Energy*, **3**, *3*, 157 (1979); https://doi.org/10.1016/0149-1970(79)90018-0.
20. A. M. WEINBERG and H. C. SCHWEINLER, "Theory of Oscillating Absorber in a Chain Reactor," *Phys. Rev.*, **74**, *8*, 851 (1948); https://doi.org/10.1103/PhysRev.74.851.

21. A. BEN-ADBENNOUR, R. EDWARDS, and K. LEE, "LQG/LTR Robust Control of Nuclear Reactors with Improved Temperature Performance," *IEEE Trans. Nucl. Sci.*, **39** (Nov. 1992).

22. F. HAGHIGHAT, T. E. UNNY, and M. CHANDRASHEKAR, "Stochastic Modeling of Transient Heat Flow Through Walls," *Trans. ASME*, **17**, 202 (1985).

23. C. DUBI and R. ATAR, "Modeling Neutron Count Distribution in a Subcritical Core by Stochastic Differential Equations," *Ann. Nucl. Energy*, **111**, 608 (2018); https://doi.org/10.1016/j.anucene.2017.09.040.

24. Z. GAJIC and M. T. J. QURESHI, "Lyapunov Matrix Equation in System Stability and Control," *Mathematics in Science and Engineering*, No. 195, Academic Press (1995).

25. E. GILAD et al., "Sensitivity of Power Spectral Density Techniques to Numerical Parameters in Analyzing Neutron Noise Experiments," *Prog. Nucl. Energy*, **101**, 288 (Nov. 2017); https://doi.org/10.1016/j.pnucene.2017.03.019.

26. P. KLOEDEN and E. PLATEN, *Numeric Solutions to Stochastic Differential Equations*, "Applications of Mathematics," Chap. 23, Springer (1992, 1995, 1999).